Home

International Journal of Energy Technology and Policy (IJETP)
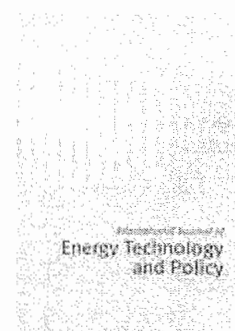
Volume 6 - Issue 1/2 - 2008

Special Issue on Computational Fluid Dynamics Simulations in Energy Technologies and Processes

Guest Editor: Professor Viorel Badescu

Table of Contents

📄 Editorial

Pages   Title and authors

Editorial

Viorel Badescu

Candida Oancea Institute,
Faculty of Mechanical Engineering,
Polytechnic University of Bucharest,
Spl. Independentei 313, Bucharest 060042, Romania
Email: badescu@theta.termo.pub.ro

Biographical note: Viorel Badescu is a Professor in the Department of Engineering Thermodynamics. His mainstream scientific contributions consist of about 200 papers and several books related to statistical physics, thermodynamics, the physics of semiconductors, various aspects of terrestrial and space solar energy applications and other energy related issues. Also, he has theorised on the present-day Mars-meteorology and -terraforming and on several macro-engineering projects. He received four awards among which the Romanian Academy Prize for Physics in 1979.

The most efficient usage of the energy resources has been challenging both in the energy industry and academia for more than 200 years. It is often difficult or impossible to experiment with the real large-scale or expensive energy production systems, to determine improved or optimal solutions. Also, analytical models of energy technology problems can only partially explain and solve real-world problems and usually, this is achieved only with significant simplifications to the models, which make them less representative in practical cases. However, with the impressive progress in computing technology, Computational Fluid Dynamics (CFD) simulation has been widely used in the recent years to model and solve energy related problems. Advanced simulation modelling techniques such as the finite element or boundary element methods have been developed and widely employed in the analysis of energy processes. Applications of CFD simulation vary widely and present a fascinating range of scenarios and techniques.

This special issue of the *International Journal of Energy Technology and Policy* is intended to present recent development and applications of CFD simulation in energy related studies. The eleven selected papers cover a broad spectrum of areas, such as energy technologies and processes associated to thermal power plant operation, renewable energy technologies, energy system analysis, energy efficiency and energy saving (applications and implications), integrated design, as well as energy transmission and distribution issues. The main scope of all these papers is to show how CFD may be used to solve various types of real-world energy problems. CFD simulation methodologies and case studies in the application of simulations are also a part of the work.

A short presentation of the papers included in this special issue follows.

- Dragos Isvoranu in his paper

  "NO_x re-burn simulation in a double-jet counter-flow flame."

presents a potential method for NO_x species reduction based on exhaust gas re-burn with air–fuel mixture in a double-jet counter diffusion flame. The most interesting outcome of the research is that NO emission index has a minimum value of depending upon the equivalence ratio of the air–methane mixture.

- Hideo Kawahara and Tatsuo Nishimura in their paper

  "Vortex structure and heat transfer in a diffusion combustion field with circulating flow."

performed a numerical study to examine the vortical structures for combusting flow from a 2D bluff-body slot burner in the transitional recirculating flow. As a result of the study, it was possible to reproduce the dynamic motions of vortical structures. In the low Reynolds number region, vortex structures in the recirculating region gives large effect in the flame shape. In addition, it was confirmed that independently of the fuel variety, the flow at the bluff-body aft comes into three shape varieties.

- Dorin Stanciu and Mircea Marinescu in their paper

  "RANS Based Numerical Simulation of External Heat Convection and Losses for Transitional Subsonic Flows through a 2D Turbine Passage."

proved that CFD became an indispensable tool for turbomachinery applications. The necessity of efficiency rising requires the development of turbulence and loss models able to correctly predict the performances of transitional fluid flow and heat transfer processes through high turning turbine blades. The paper analyses the behaviour of the most advanced eddy diffusivity turbulence closure model to simulate these kinds of flows and propose a new model of loss evaluation based on the second law of thermodynamics. The model, which uses the volumetric rate of entropy generation as a loss measure, has the advantage of locally revealing the exergy dissipations in every peculiar zone of the flow, like boundary layer, wake, recirculation bubble zone, etc.

- Gabriel P. Negreanu in his paper

  "Numerical simulation of a large power steam turbine run-up."

presents a differential approach of the fluid dynamic processes occurring in the flow path of a large power steam turbine during run-up period. The simulation is performed by the numerical integration of ordinary differential equations obtained by applying the laws of mass and energy conservation in turbine's internal cavities. In this manner, the turbine power and rotor speed vs. time function of the aperture law of the start-up valve have been obtained.

- C. Luca Iandoli, Enrico Sciubba and Nicola Zeoli in their paper

  "The computation of the entropy generation rate for turbomachinery design applications: some theoretical remarks and practical examples."

present a rather complete and accurate, albeit general, analysis of the importance of the local entropy generation maps for turbomachinery applications. The authors argue that the information provided by the separate calculation of the viscous and thermal components of the entropy generation provide designers with an invaluable additional insight into the flow phenomena and on the related irreversibilities. A detailed theoretical discussion is presented, with some preliminary remarks on the approximations introduced

by the turbulence models. Several examples of CFD calculations of the entropy generation in realistic 2- and 3D turbomachinery stages are presented and discussed.

- Triwahju Hardianto, Nobuomi Sakamoto and Nobuhiro Harada in their paper

  "Computational study of a diagonal channel magnetohydrodynamic power generation."

study the performance of a diagonal conducting wall channel Magnetohydrodynamic (MHD) power generation. As a model, the authors are using a scramjet-driven MHD generator channel. It is found that the combustion efficiency of 95% yields a better power generation than 85 and 75% combustion efficiencies.

- Alexandru M. Morega et al. in their paper

  "A Finite Element Method Analysis and Optimization of a Polymer Electrolyte Membrane Fuel Cell with Interdigitated Flow Field Design."

show that Interdigitated Polymer Electrolyte Fuel Cells are particularly attractive due to the enhanced transport rates and benefits with respect to electrode flooding. A 2D isothermal finite element model is used to simulate the outlining processes that occur at the elemental fuel cell level, and to identify potential design enhancement opportunities. The authors outlined an optimal size of the elemental gas channel inlet/outlet width, for fixed elemental cell height, such that the total electrical power of the elemental cell (hence, the total cell/stack electrical power) is maximised, under a constant pressure drop constraint.

- Radu D. Rugescu in his paper

  "Technology of CFD in space engines and solar-gravity draught power plants."

presents the original unsteady numerical code TRANSIT as well as the first results of the flow simulation of a starting transient in the gravitational draught tower WINNDER for aero-acoustic experiments. First, developed to calculate starting transients in rocket engines, TRANSIT 1D method also covers the non-isentropic and discontinuous flow regions with high and equal accuracy within tall gravity draught solar towers. The fresh air in the WINNDER tunnel is heated through a new system of solar mirror arrays and numerical simulations show an unexpected stepwise initial acceleration of the air along this tower, despite the continuous variation of the air temperature itself.

- T. Kousksou et al. in their paper

  "Numerical simulation of fluid flow and heat transfer in a phase change thermal energy storage"

studied an industrial process of energy storage. The authors developed a 2D numerical model. They used a porous medium approach and considered the super-cooling phenomenon. The system consists of a cylindrical tank filled with encapsulated liquid–solid Phase Change Materials. The effects of different parameters on the behaviour of the tank, such as capsule size, porosity of the packed capsules and the tank dimension were examined when the tank is in horizontal position.

- Milorad Bojic, Slobodan Savic and Danijela Nikolic in their paper

  "Application of CFD to flow next to high-rise buildings in Hong Kong due to air-conditioner heat rejection"

review CFD studies of flow field and temperature next to high-rise residential buildings. This flow field, established by a number of window air-conditioners that reject condenser heat into their recessed spaces, is investigated by using FLUENT 5.0 and k–ε turbulence model. The research is performed for different high-rise buildings with different condenser-unit locations.

- Kaveh Sookhak Lari in his paper

  "Thermal Energy Flow Modelling in a Typical University Classroom"

shows that despite the low energy price in Iran, saving energy policies are important in several fields such as buildings, transportation and public issues. As an applied project, the Isfahan University of Technology decided to evaluate existing energy consumption situation of the campus buildings. As a part of this project, the author simulated thermal energy flow in a typical classroom and suggested some modifications to improve the efficiency.

Application of Computational Fluid Dynamics to flow next to high-rise buildings in Hong Kong due to air-conditioner heat rejection

M. Bojic*, S. Savic and D. Nikolic

Faculty of Mechanical Engineering at Kragujevac,
University of Kragujevac,
Sestre Janjic 6,
34000 Kragujevac, Serbia
Fax: +381 34 330196
E-mail: bojic@kg.ac.yu   E-mail: ssavic@kg.ac.yu
E-mail: danijelan@kg.ac.yu
*Corresponding author

Abstract: This paper presents the results of several studies done for high-rise residential buildings in Hong Kong that involved Computational Fluid Dynamics (CFD) simulation. During summer, a number of Window Air-Conditioners (WACs) could be rejecting condenser heat into a recessed space of these high-rise residential buildings. FLUENT 5.0, a CFD code can be used to predict temperatures and flow field of a powerful rising hot air stream formed in the recessed space. In these cases, for simulations, we use k–ε turbulence model, and 2D and 3D model of the building. A CFD code can also be used to predict temperature and flow fields inside the recessed spaces that differ in heights and condenser-unit locations. The CFD code 'FLUENT' is also employed to predict the airflow patterns. The papers study the worst-case scenario in summer when all the WAC units reject condenser heat into this space.

Keywords: Computational Fluid Dynamics; CFD; heat rejection; high-rise residential buildings; recessed spaces; temperature rise; Window Air-Conditioners; WACs.

Reference to this paper should be made as follows: Bojic, M., Savic, S. and Nikolic, D. (2008) 'Application of CFD to flow next to high-rise buildings in Hong Kong due to air-conditioner heat rejection', *Int. J. Energy Technology and Policy*, Vol. 6, Nos. 1/2, pp.159–177.

Biographical notes: Milorad Bojic finished Mechanical Engineering at Belgrade University, Yugoslavia, MSc at Syracuse University, New York, USA and Sci.Dr. at Kragujevac University, Yugoslavia. He is a Full Professor of Mechanical Engineering and Director of Centre for Heating, Air Conditioning and Solar Energy at Kragujevac University. During the years 1997 and 2001–2002, he was a Visiting Professor at Nagoya University, Japan. In 2002/2003, he was a Honorary Professor at Hong Kong Polytechnic University. He is an author of more than 200 scientific papers. He is an Elected Member of Serbian Scientific Society and of Serbian Academy of Engineering Sciences.

Slobodan Savic finished Mechanical Engineering, MSc and Sci.Dr. at Kragujevac University. He worked as an Assistant Candidate, an Assistant and now he is an Assistant Professor at the Faculty of Mechanical Engineering in

Kragujevac, Department of Applied Mechanics and Automatic Control. He is an author of 15 scientific papers in international and domestic journals. He has participated in realisation of six scientific-research projects. He is a co-author of a university textbook titled hydraulics – basics.

Danijela Nikolic finished Mechanical Engineering at Kragujevac University. Since October 2000, she worked as an Assistant Candidate at the Faculty of Mechanical Engineering in Kragujevac, Department of Energy and Process Engineering. She is an author of 12 scientific papers in international and domestic journals. She has participated in realisation of seven scientific-research projects.

Nomenclature

C_1, C_2, C_e,	constants of the turbulence model
D	depth (m)
Dt	temperature rise (°C)
g	gravitational acceleration (m sec^{-2})
G	separation distance of two vertical sidewalls (m)
Gr	Grashof number
h	height inside the recessed space (m)
H	height, high part of a recessed space (m)
K	non-dimensional turbulent kinetic energy
L	characteristic length (m)
m	mass-flow rate (kg sec^{-1})
n	number of horizontal plates
N	number of condenser units
p	pressure (Pa)
p_∞	pressure inside free stream (Pa)
P	electricity consumption rate (W) non-dimensional pressure, potential for cross-ventilation
Pr	Prandtl number
Q	cooling capacity rate (W)
Re	Reynolds number
Ra	Rayleigh number
t	temperature (K)

Δt	elevation in the entering condenser air temperature, temperature rise (K)
T	non-dimensional temperature
u, v, w	velocities (m sec^{-1})
U, V, W	non-dimensional velocities
W	width
x, y, z	lengths (m)
X, Y, Z	non-dimensional lengths

Greek letters

α_t	non-dimensional turbulent thermal diffusivity (m^2 sec^{-1})
β	thermal expansion coefficient (1/K)
ε	non-dimensional dissipation rate of the turbulent kinetic energy
ν_t	turbulent kinematic viscosity (m^2 sec^{-1})
ρ	air density (kg m^{-3})
$\sigma_\varepsilon, \sigma_K$	constants in the turbulence model
τ	non-dimensional time

Subscripts

av	average
b	bulk-flow, mainstream of the buoyant stream
c	average for condensers, condenser unit
e	entering, entrainment
f	free environment, front
fo	ordinary facet
fs	small facet
i	opening facing the corner wall, inner air-conditioner
j	number of Window Air-Conditioners and number of story
m	mass-weighted, maximum, minimum
o	opening facing the outdoor, outer air-conditioner
t	turbulence quantities
∞	free stream

1   Introduction

High-rise residential buildings in Hong Kong have the special shape (Figure 1). They have the outdoor recessed spaces formed by pairs of adjacent residential units that extend outward from a central core. They allow individual residential units to have more external walls and windows. This helps to maximise the availability of daylight and natural ventilation to the units. In addition, plumbing and drainage pipes may be installed at all the external side of the wall within the recessed space to ease maintenance and repair.

Figure 1   High-rise residential buildings in Hong Kong

For a high-rise residential building in Hong Kong, there could be a pile of more than 100 Window Air-Conditioners (WACs) simultaneously rejecting condenser heat into a recessed space, which acts as a chimney. In calm days, the condenser units of WACs on the top floors will draw less air at an elevated ambient air temperature due to heat rejection of air-conditioners below. An air-conditioner will consume more electricity for producing the same amount of cooling, its cooling capacity may be de-rated, and its operation may be interrupted. This phenomenon should be taken into consideration while designing residential buildings to minimise its adverse effect, ensure sufficient cooling capacity and minimise electricity use of air-conditioners. The window-type air-conditioners are studied because it is customary in Hong Kong to be used in low-income public housing, where as the split-type air-conditioners are more often found in higher income housing.

   The influence of the air-conditioners exhausts into the recessed space to their performance was researched for both types of air-conditioners by using Computational Fluid Dynamics (CFD) approach. The split-type was investigated by Chow and Lin (1999) and Chow, Lin and Wang (2000) and the window-type by Bojic, Yik and Lee (2001, 2002, 2003). The CFD approach was used for these investigations due to the following reasons. Due to complexity and large scale of a recess, investigations of the flow inside the recessed space cannot be adequately performed by field or laboratory measurements, and the CFD simulations are the best way to go. During the field measurements, it is almost impossible to control and monitor environmental conditions

and condenser-unit operation. During the laboratory measurements, it is next to impossible to scale condenser units and to achieve satisfactory measurement accuracy. The CFD simulations enable the most economical, fast, and flexible study of this problem.

This paper would review the researches carried out (Bojic, Yik and Lee, 2001, 2002, 2003) on WACs in a recessed space of the Hong Kong high-rise buildings. These simulations were done for the worst-case scenario when all WACs operated simultaneously at the full load without wind to disperse hot air in the recessed space. The CFD predictions reveal that the recessed space is characterised by a very complex flow and temperature pattern governed by buoyancy, momentum, and confinement of the inside air streams. Buoyancy, that drives air toward upper stories of the building, is generated by intensive hot air exhausts from condenser units. To simplify the simulation analysis, all condensing units have the same dissipation rate, and all their fans have the same characteristics, all wall surfaces of the recessed space are adiabatic, plane, and without openings and impermeable. The environment air outside of the recessed space has the same temperature regardless of the height of the recessed space, and the effect of solar radiation on the wall surface of the recessed space is not taken into account.

2   Mathematical model: CFD development

WACs can cause rather complicated flow field patterns outside the building in the recessed space; then, three heat transfer phenomena may be noticed:

1   forced convection by the condenser fans

2   a mixture of forced and natural convection

3   natural convection by thermal buoyancy generated by rejected condenser heat.

The flow pattern is governed by the conservation principles of fluid motion and heat transfer, namely conservation of mass, momentum, and energy. It is assumed that the air density changes as a result of heat input, and the Boussinesq approximation applies, which is the most commonly used model in solving natural convection problems as suggested by Costa, Oliveira and Blay (1999). This model involves conceptually two assumptions:

1   it neglects all the variable-property effects in the governing equations, except for the density in the momentum equation

2   it approximates the density difference term with a simplified equation as follows:

$$\rho_\infty - \rho = \rho\beta(t - t_\infty) \tag{1}$$

where ρ stands for the air density, ρ_∞ stands for the density of the free air stream, t stands for temperature, t_∞ stands for temperatures of the free air stream, and β stands for the coefficient of thermal expansion.

The importance of the buoyancy forces in this kind of problems can be measured by the ratio of the Grashof (*Gr*) number to the square of the Reynolds (*Re*) number

$$\frac{Gr}{Re^2} = \frac{\beta(t - t_\infty)gL}{u^2}. \tag{2}$$

In this equation, g is the gravitational acceleration, L is the characteristic length and u is the characteristic velocity. When this ratio approaches or exceeds unity, strong buoyancy effects are expected. Conversely, if it is very small, buoyancy forces may be ignored in the simulation.

The turbulent flow solution applied in this case includes the use of the two-equation k–ε model, which is based on the concept of eddy viscosity to account for the additional Reynolds stresses terms found in the Reynolds-Averaged-Navier-Stokes (RANS) equations. Launder and Spalding (1974) and then Chen and Jiang (1992) used this model in studies on the turbulent natural convection flow. The model can be expressed by the equations that follow.

The continuity equation

$$\frac{\partial U}{\partial X} + \frac{\partial V}{\partial Y} + \frac{\partial W}{\partial Z} = 0. \tag{3}$$

The X-momentum equation

$$\frac{\partial U}{\partial \tau} + U\frac{\partial U}{\partial X} + V\frac{\partial U}{\partial Y} + W\frac{\partial U}{\partial Z} = Pr\left\{\frac{\partial}{\partial X}\left[(1+\nu_{\mathrm{t}})\frac{\partial U}{\partial X}\right] + \frac{\partial}{\partial Y}\left[(1+\nu_{\mathrm{t}})\frac{\partial U}{\partial Y}\right]\right.$$
$$\left. + \frac{\partial}{\partial Z}\left[(1+\nu_{\mathrm{t}})\frac{\partial U}{\partial Z}\right]\right\} - \frac{\partial P}{\partial X}. \tag{4}$$

The Y-momentum equation (Y being the vertical direction)

$$\frac{\partial V}{\partial \tau} + U\frac{\partial V}{\partial X} + V\frac{\partial V}{\partial Y} + W\frac{\partial V}{\partial Z} = Pr\left\{\frac{\partial}{\partial X}\left[(1+\nu_{\mathrm{t}})\frac{\partial V}{\partial X}\right] + \frac{\partial}{\partial Y}\left[(1+\nu_{\mathrm{t}})\frac{\partial V}{\partial Y}\right]\right.$$
$$\left. + \frac{\partial}{\partial Z}\left[(1+\nu_{\mathrm{t}})\frac{\partial V}{\partial Z}\right]\right\} - \frac{\partial P}{\partial Y} + RaPrT. \tag{5}$$

The Z-momentum equation

$$\frac{\partial W}{\partial \tau} + U\frac{\partial W}{\partial X} + V\frac{\partial W}{\partial Y} + W\frac{\partial W}{\partial Z} = Pr\left\{\frac{\partial}{\partial X}\left[(1+\nu_{\mathrm{t}})\frac{\partial W}{\partial X}\right] + \frac{\partial}{\partial Y}\left[(1+\nu_{\mathrm{t}})\frac{\partial W}{\partial Y}\right]\right.$$
$$\left. + \frac{\partial}{\partial Z}\left[(1+\nu_{\mathrm{t}})\frac{\partial W}{\partial Z}\right]\right\} - \frac{\partial P}{\partial Z}. \tag{6}$$

In Equations (3)–(6), U, V and W are the non-dimensional velocities, X, Y and Z are the non-dimensional lengths, τ is the non-dimensional time, Pr is the Prandtl number, Ra is the Rayleigh number, T is the non-dimensional temperature, P is the non-dimensional pressure, and ν_{t} is the turbulent kinematic viscosity.

The energy equation

$$\frac{\partial T}{\partial \tau} + U\frac{\partial T}{\partial X} + V\frac{\partial T}{\partial Y} + W\frac{\partial T}{\partial Z} = \frac{\partial}{\partial X}\left[(1+\alpha_{\mathrm{t}})\frac{\partial T}{\partial X}\right] + \frac{\partial}{\partial Y}\left[(1+\alpha_{\mathrm{t}})\frac{\partial T}{\partial Y}\right]$$
$$ + \frac{\partial}{\partial Z}\left[(1+\alpha_{\mathrm{t}})\frac{\partial T}{\partial Z}\right]. \tag{7}$$

The turbulent kinetic energy equation

$$\frac{\partial K}{\partial \tau} + U\frac{\partial K}{\partial X} + V\frac{\partial K}{\partial Y} + W\frac{\partial K}{\partial Z} = Pr\left\{\frac{\partial}{\partial X}\left[\left(1+\frac{v_t}{\sigma_K}\right)\frac{\partial K}{\partial X}\right] + \frac{\partial}{\partial Y}\left[\left(1+\frac{v_t}{\sigma_K}\right)\frac{\partial K}{\partial Y}\right]\right.$$

$$+ \frac{\partial}{\partial Z}\left[\left(1+\frac{v_t}{\sigma_K}\right)\frac{\partial K}{\partial Z}\right]\right\} + Prv_t\left[\left(\frac{\partial U}{\partial Y}+\frac{\partial V}{\partial X}\right)^2\right.$$

$$+ \left(\frac{\partial V}{\partial Z}+\frac{\partial W}{\partial Y}\right)^2 + \left(\frac{\partial W}{\partial X}+\frac{\partial U}{\partial Z}\right)^2 + 2\left(\frac{\partial U}{\partial X}\right)^2$$

$$\left.+ 2\left(\frac{\partial V}{\partial Y}\right)^2 + 2\left(\frac{\partial W}{\partial Z}\right)^2\right] - \varepsilon - v_t Ra\frac{Pr^2}{Pr_t}\frac{\partial T}{\partial X}. \tag{8}$$

The dissipation of turbulent kinetic energy equation

$$\frac{\partial \varepsilon}{\partial \tau} + U\frac{\partial \varepsilon}{\partial X} + V\frac{\partial \varepsilon}{\partial Y} + W\frac{\partial \varepsilon}{\partial Z} = Pr\left\{\frac{\partial}{\partial X}\left[\left(1+\frac{v_t}{\sigma_\varepsilon}\right)\frac{\partial \varepsilon}{\partial X}\right] + \frac{\partial}{\partial Y}\left[\left(1+\frac{v_t}{\sigma_\varepsilon}\right)\frac{\partial \varepsilon}{\partial Y}\right]\right.$$

$$+ \frac{\partial}{\partial Z}\left[\left(1+\frac{v_t}{\sigma_\varepsilon}\right)\frac{\partial \varepsilon}{\partial Z}\right]\right\} + C_1 Pr\frac{\varepsilon}{K}\left[\left(\frac{\partial U}{\partial Y}+\frac{\partial V}{\partial X}\right)^2\right.$$

$$+ \left(\frac{\partial V}{\partial Z}+\frac{\partial W}{\partial Y}\right)^2 + \left(\frac{\partial W}{\partial X}+\frac{\partial U}{\partial Z}\right)^2 + 2\left(\frac{\partial U}{\partial X}\right)^2$$

$$\left.+ 2\left(\frac{\partial V}{\partial Y}\right)^2 + 2\left(\frac{\partial W}{\partial Z}\right)^2\right] - C_2\frac{\varepsilon^2}{K} - C_e v_t Ra\frac{\varepsilon}{K}\frac{Pr^2}{Pr_t}\frac{\partial T}{\partial X}. \tag{9}$$

In Equations (7)–(9), α_t is the non-dimensional turbulent thermal diffusivity, K is the non-dimensional turbulent kinetic energy, ε is the non-dimensional dissipation rate of the turbulent kinetic energy, σ_ε and σ_K are the constants in the turbulence model, Pr_t is the turbulent Prandtl number and C_1, C_2, C_e are the constants of the turbulence model.

The commercial finite volume-based CFD code, FLUENT 5.0, is used to simulate the mixed convection flow problem of heat rejection from the condenser of WACs, as stated in user manual (Anonymous, 2000). Vandoormaal and Raithby (1984) used a segregated solver based on the Semi-Implicit Method for Pressure-Linked Equations-Consistent algorithm as the pressure–velocity coupling scheme and the Boussinesq approximation. All the discretised scalar equations, including three momentum, one energy, and one turbulence kinetic energy equations, are determined using the second-order upwind interpolation scheme. Steady-state solutions are obtained by a time-dependent approach in which the convergence is judged by considering the residual level of the governing equations and convergence of other integrated heat transfer quantities such as the total heat flux and average temperature on certain cross-sectional planes.

In the simulation setup, we present the WAC condenser by using an adiabatic casing, a heat-exchanger coil, and a propeller-type fan. Yik (2000) uses empirical models for the split-type air conditioners to predict the influence of the entering condenser air temperature t_e on the performance of the air-conditioner, which includes the actual rate of its electricity consumption P and the actual cooling capacity Q.

To analyse flow and heat transfer inside the recessed space and condenser units, we allocate a computational domain, divide this domain into control volumes, and use conservation equations on each control volume. The computational domain comprises of 490,185 control volumes.

3   Simulation

To run a computer simulation, one would establish the geometry of the studied recessed space, of the condenser position in the space, and of each condenser unit. Then, one would exploit the FLUENT graphical capabilities to generate the computational geometry and to create the computational mesh. Furthermore, one would establish simulation parameters of all condenser units inside the entire recessed space as well as the environmental conditions.

1   Bojic, Yik and Lee (2001, 2002, 2003) studied recessed spaces for a 12- and 30-storied building. The layout plan of the studied recessed spaces of 'I' type for a high-rise residential building is shown in Figure 2. The recessed space represents a big vertical shaft that exists outside the building; the shaft is shaped by two vertical sidewalls and one vertical corner wall. The shaft is characterised by three distances:

    i   the separation distance ($G = 3$ m) of two vertical sidewalls (the width of the recessed space)

    ii   distance ($D = 6$ m) between the corner wall and the non-recessed space (depth of the recessed space)

    iii height of the recessed space. As the floor-to-ceiling distance for one-story is 3 m, the height of the investigated recessed spaces would be $H = 36$ for the 12-storied building, and 90 m for the 30-storied buildings. Bojic, Yik and Lee (2003) also investigated the recessed space that may contain one or two horizontal plates.

2   Bojic, Yik and Lee (2001, 2002, 2003) studied the recessed space, with four or one window-type air-conditioner per story. For the first case, two of the condensers mounted on one sidewall face, and the other two condensers mounted on the opposite sidewall. The corner wall is without WACs. For the second case, one of the condensers is mounted on one of the sidewall faces.

3   Every WAC has three openings in the recessed space: two side openings where air enters the WAC condenser, and one front opening where this air exits the condenser. These side openings may face either the building (designated as the inner-side openings) or the opposite of the building (designated as the outdoor-side openings). The casing of the unit is 0.5 m in depth, 0.5 m in width, and 0.45 m in height.

4   The simulation parameters of the recessed space and the condensing units are the following.

    •   All WACs inside the recessed space simultaneously operate in the full load, which is the worst operating condition for the recessed space.

    •   Every condensing unit dissipates 4 kW of heat.

- Every fan inside the condensing unit generates a pressure head of 3 Pa to enable the airflow rate of 0.2453 kg sec^{-1} through the condensing unit under nominal conditions.

- The outdoor air is assumed to be still, to have a temperature of 27.15°C (300 K) and a low turbulence intensity of 1%. These values do not change with the height of the recessed space.

5   For the recessed space, we have assumed that the wall surfaces of the recessed space are flat and do not contain any opening. We have also assumed that wall surfaces are adiabatic and that they are not affected by solar radiation.

6   We studied the worst-case scenario in summer when all the WAC units reject condenser heat into this space.

Figure 2   Layout of the recessed space of a high-rise residential building
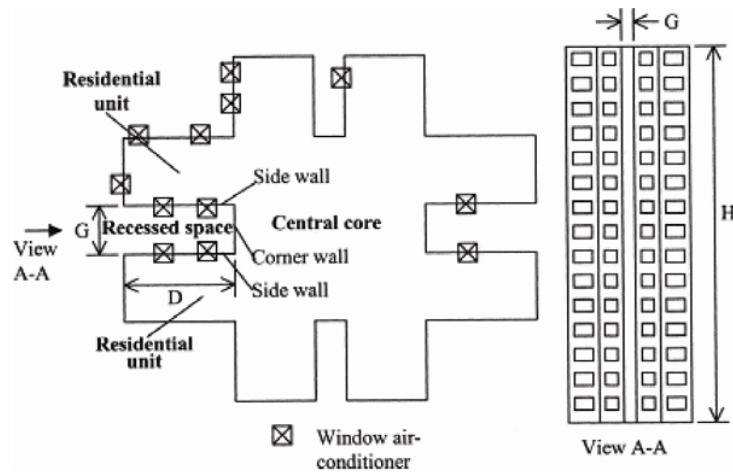
Source: Bojic, Lee and Yik (2001). Copyright (2001), with permission from Elsevier.

4   Results and analyses

Bojic, Yik and Lee (2001, 2002, 2003) studied the application of CFD to flow next to high-rise buildings due to the WAC heat rejection. Here, we present their results, analyses, and conclusions.

4.1   Flow and temperature field in the recessed space

To determine horizontal and vertical non-uniformity of flow and temperature field inside the I-shaped recessed space, Bojic, Yik and Lee (2001) present the results of the study on heat rejection by a large number of the condensers of WACs (four per story) into a 12- and 30-storied high recessed space.

The detailed horizontal non-uniformity of temperature distribution in Figure 3a shows existence of vortices inside the upstream flow field in the recessed space. This reveals one strong horseshoe bulk air stream and two strong vortices located inside the inner region, which is the hottest part of the recessed space. Although this bulk air stream is generated by buoyancy, these vortices may also be responsible for the entertainment of some air from the outside to the recessed space.

Figure 3   Temperatures for the airflow exiting the 15th story recessed space and entering the 16th story recessed space at the horizontal planes for case 1
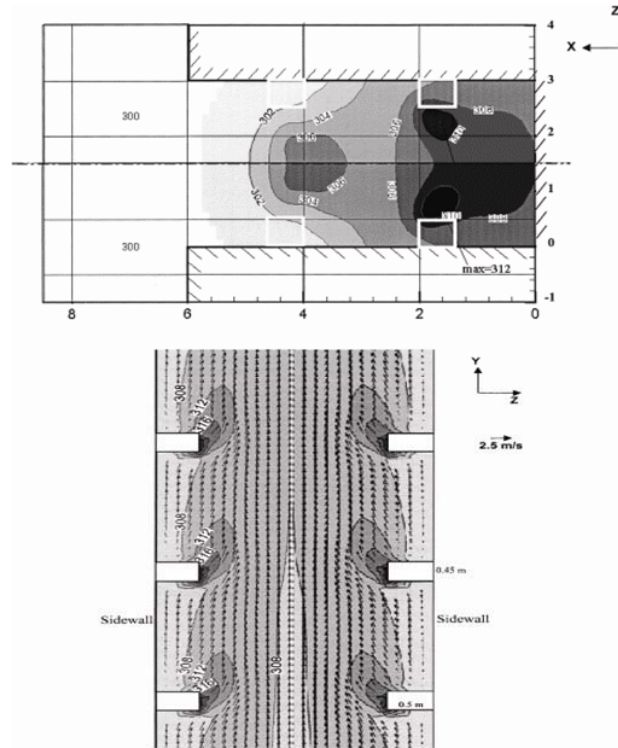
Velocity vectors and temperature contours in the vertical symmetry plane $X = 1.75$ m for case 1 and the 30-storied building. The recessed spaces of 15, 16, and 17th stories are shown. All temperatures are in K.

Source: Bojic, Lee and Yik (2001). Copyright (2001), with permission from Elsevier.

The detailed vertical non-uniformity in temperature distributions and flow development in the recessed space, shown in Figure 3b, reveals very powerful bulk stream going upstream in the recessed space. The condenser unit located closer to the core of the hot air stream may draw less air at higher temperature. The maximum temperature elevation recorded is 11°C. The minimum mass-flow rate recorded is 22% lower than the condenser nominal mass-flow rate.

4.2   *Flow and temperatures of the bulk flow in the recessed space*

To determine flow and temperatures of the vertical bulk flow inside the I-shaped recessed space, Bojic, Yik and Lee (2003) present the results of the study on heat rejection by a large number of the condensers of WACs into a 12- and 30-storied high recessed space (four per story). For the bulk flow, Figure 4a shows its mass-flow rate m_{av}, and Figure 4b its temperature rise Δt_{av}. These figures show that m_{av}, and Δt_{av} increase with the height of the recessed space. The air entrainment into the bulk air stream decreases with this height. Furthermore, these figures show that the values in the m_{av} and Δt_{av} for the top story of the 30-storied building are considerably higher than that for the top story of the 12-storied building. The condenser unit located higher draw less air at higher temperature.

Figure 4   (a) Mass-flow rate of air and its entrainment in the recessed space as a function of the building height. Diagrams are given for case 2 and for the 12- and 30-storied buildings
(b) The temperature rise vs. building height for the 12 and 30-storied buildings
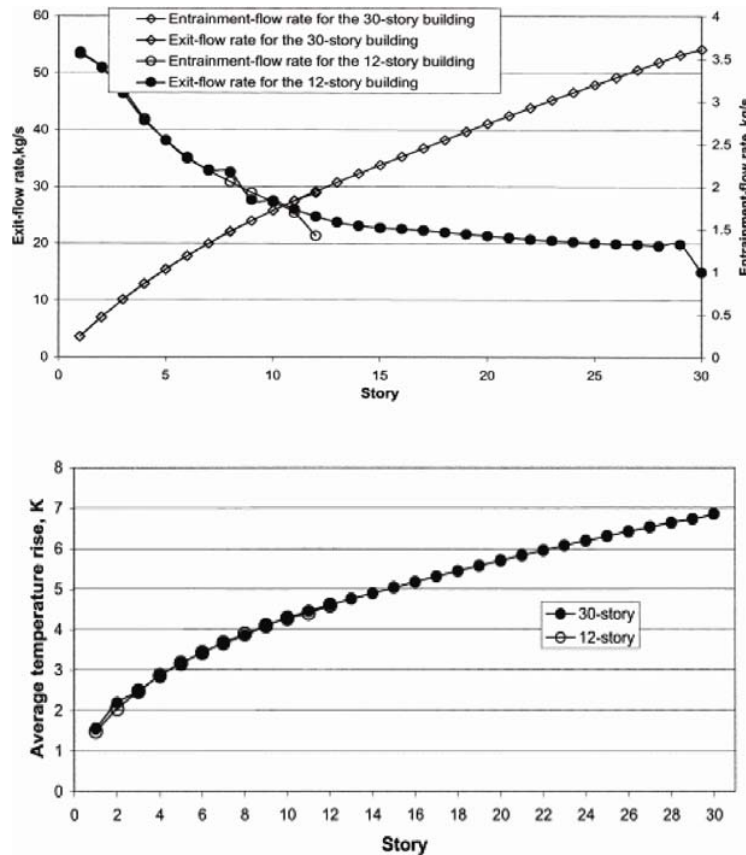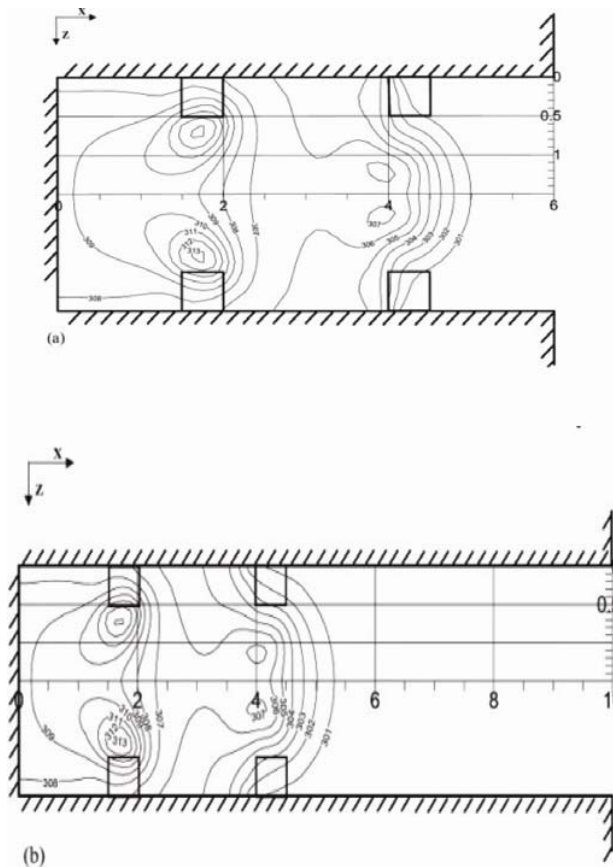
4.3 *Horizontal development of flow and temperature field with depth of a recessed space*

Bojic, Yik and Lee (2002) show how the depth of the I-shaped 30-story recessed space (120 condenser units – four condenser units per story) influences the detailed horizontal temperature development inside this recessed space. Two depths are investigated: $D = 6$ m (the shallow recessed space), and $D = 10$ m (the deep recessed space).

To compare its detailed horizontal temperature development inside the bulk buoyant flow for both the recessed spaces, we report detailed distributions of the temperature in a horizontal imaginary plane $Y = 60$ m at the ceiling level of the recessed space belonging to the 20th story perpendicular to the bulk flow. It is found by an inspection of the calculated results that, in most of the ceiling planes, these distributions have similar shape. When defined by using the temperature contours, the flow region inside the deep recessed space is slightly larger than that inside the shallow recessed space (Figure 5).

Figure 5   Temperatures (K) for the airflow at $Y = 60$ m: (a) shallow and (b) deep recessed space

Source: Bojic, Lee and Yik (2002). Copyright (2002), with permission from Elsevier.

4.4   Bulk flow with depth of a recessed space – vertical development

Bojic, Yik and Lee (2002) show how the depth of the I-shaped 30-story recessed space with 120 condenser units influences the bulk buoyant airflow. Two investigated depths are $D = 6$ m (the shallow recessed space), and $D = 10$ m (the deep recessed space). For shallow and deep recessed space, we compare the average upward development (average mass-flow rates and temperature rises) of the buoyant airflow.

   Two average mass-flow rates that will be compared are

1   its mainstream mass-flow rate (m_b)

2   entrainment-stream mass-flow rate (m_e) (Figure 6a).

Figure 6   (a) Mainstream mass-flow rate and entrainment-flow rate, and (b) air temperature rise
for different stories and for shallow and deep recessed space
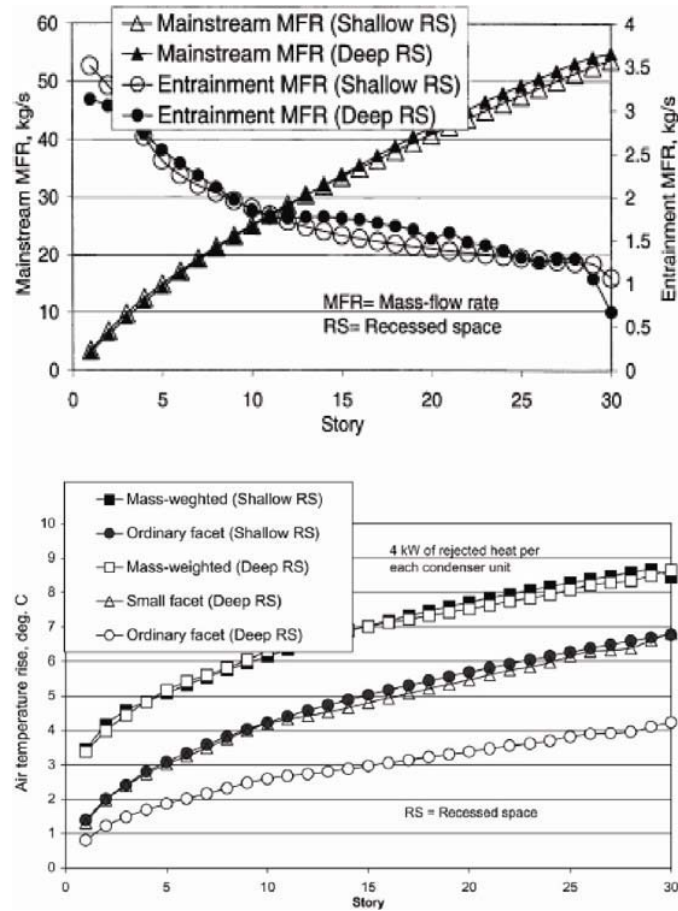
Source: Bojic, Lee and Yik (2002). Copyright (2002), with permission from
Elsevier.

For each variable, 30 values are calculated, one for each story. It is found that the deeper recessed space marginally influence m_b and m_e.

Three average temperature-rises that will be compared are

1   facet temperature rise (Δt_{fo})

2   small facet temperature rise (Δt_{fs})

3   mass-weighted temperature rise (Δt_m) (see Figure 6b).

For each variable, 30 values are calculated, one for each story. It is found that deeper recessed space considerably decreases Δt_{fo}, and does not influence Δt_{fs} and Δt_m.

4.5   *Flows to condensers with depth of a recessed space – vertical development*

Bojic, Yik and Lee (2002) show how the depth of the I-shaped 30-story recessed space influences the mass-flow rate and temperature rise of the airflow entering the condenser units. The investigated depths are $D = 6$ m (the shallow recessed space), and $D = 10$ m (the deep recessed space).

The mass-flow rates for the flow entering each of 60 inner condenser-units (m_i) and 60 outer condenser units (m_o) are compared for shallow and deep recessed space. Deeper recessed space does not vary m_i, but it influences m_o; this yields lower difference in between m_i and m_o.

For shallow and deep recessed space, three types of the temperature rise for air entering through condenser units are calculated (Figure 7). These are

1   the temperature rise for air entering two inner condenser unit existing at each story (Δt_i)

2   the temperature rise for air entering two outer condenser units existing at each story (Δt_o)

3   the temperature rise for air entering four condenser units (two inner unit and two outer units) existing at each story (Δt_c).

These variables stand for the average temperature rise above t_a in air entering these units. Deeper recessed space would influence that the inner condenser units draw the colder air (Δt_i is lower), and the outer condenser units draw the hotter air from the recessed space (Δt_o is higher). For both the recessed spaces, it may be seen that the depth of the recessed space does not change Δt_c.

Figure 7   Condenser air temperature rise for inner and outer condenser unit and shallow and deep recessed space as a function of story where this unit is located
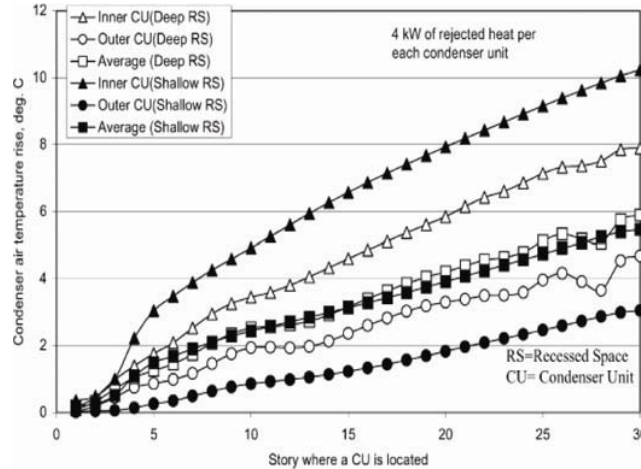
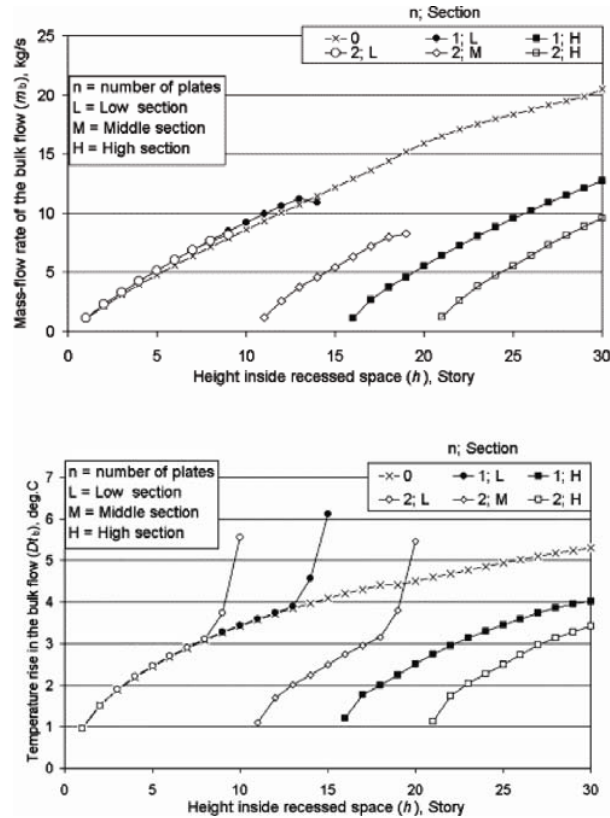### 4.6   Influence of plates on the bulk, buoyant airflow inside the recessed space

For a 30-story residential building, Bojic, Yik and Lee (2003) study the flow and temperature developments for the bulk airflow inside an I-shaped recessed space. This airflow is generated by heat rejected from 30 WACs (one per story). Total rejected heat is 120 kW. This investigation develops a new low-cost technology that uses horizontal plates to direct the hot buoyant air stream to the outside and to draw a relatively cold air stream from the outside to the inside of this recessed space. The studied recessed space is with one and two plates, and without any plate.

For the buoyant, bulk airflows by using CFD, we report their average mass-flow rates (m_b) in Figure 8a, and average temperatures (Dt_b) in Figure 8b as functions of (h) and (n). Variable h represents the height inside the recessed space (given as the number of stories from the ground) and n number of plates. Variable Dt_b represents a difference in the average temperature of air at the imaginary ceiling surface of the single-story recess and the temperature of the free environment t_f.

Figure 8a shows that for each section of the recessed space m_b increases with h from a value slightly above zero to a maximum value. Note that the lower values of m_b may mean better operation of the condensers. Variable m_{ba} decreases with n. For instance, this value for the recessed space with one plate would be lower by up to 43% and for the recessed space with two plates by up to 60% than that for the recessed space without any plate. To conclude, the condenser units in the recessed spaces with plates, on average, would have a lower exposure to the hot bulk airflow than that in the recessed space without any plate. Figure 8b shows that the temperature rise in the bulk, buoyant flow would decrease on average when the recessed space has plates. In conclusion, the horizontal plates clearly stop the vertical buoyant streams to propagate from lower sections into the upper sections of the recessed space and enable the upper sections to

draw highly diluted hot air (a mixture of hot and fresh air) instead of undiluted hot air. This would boost the performances of WACs in upper sections but would diminish the performance of the top WACs in lower sections.

Figure 8   (a) Mass-flow rate (m_b) and (b) average temperature rise (Dt_b) of the bulk flow as a function of the height (h) inside the recessed space

4.7   Influence of plates on the flow – flow of air through condenser units

For a 30-story residential building, Bojic, Yik and Lee (2003) study the flow and temperature developments for the condenser-unit airflows inside an I-shaped recessed space. These airflows are generated by heat rejected from 30 WACs (one per story). Each condenser unit is represented by a rectangular box. Total rejected heat is 120 kW. This paper investigates the possibility to develop a new low-cost technology that uses horizontal plates to direct the hot buoyant air stream to the outside and to draw relatively cold air stream from the outside to the inside of this recessed space. The recessed space is without plates (a reference case), and with one and two plates.

For the airflows in all the 30 condenser units, we report two variables obtained by CFD in Figures 9a and b. In Figure 9a, the average condenser mass-flow rate (m_c) is given as a function of (h) and (n). In Figures 9b, the average temperature rise (Dt_c) at the entrance of this airflow to the condenser is given as a function of (h) and (n). Variable h represents the height inside the recessed space (given as the number of stories from the ground) and variable n represents the number of plates.

Figure 9a shows that the mass-flow rate of air entering the condenser coils, on average, substantially increases with a provision of plates inside the recessed space, which is beneficial to the condenser units. However, for the low-level units, the mass-flow rate slightly decreases. Figure 9b shows that the temperature rise in air entering the condenser coils, on average, substantially decreases with placement of plates. Then, the condenser coils would benefit. However, for WACs located at low and middle section, the first condenser units below the plates would suffer.

Figure 9   (a) Mass-flow rate (m_c) through a condenser unit and (b) temperature rise (Dt_c) in air entering the condenser unit as a function of the unit height (h) above ground
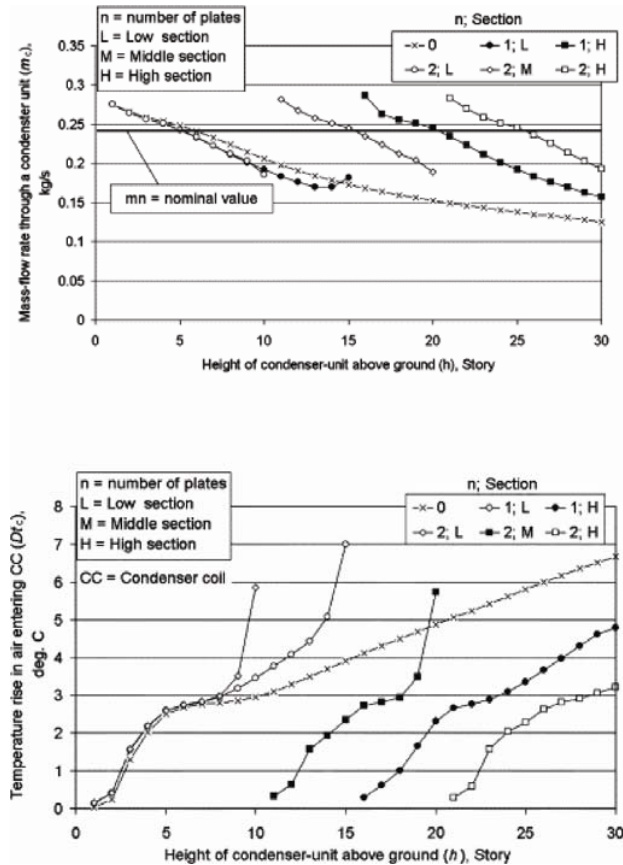
5   Conclusion

The predictions by using FLUENT 5.0, a CFD code, show the following. Generally, WACs in the recessed space may experience two basic situations. In the first situation, the condenser air may have the mass-flow rate lower than the nominal and may have the temperature higher than that of the outdoor air. Then, energy losses would occur. In the second situation, condenser air may have the mass-flow rate higher than nominal and may have the temperature higher than that of the outdoor air. Then, an energy benefit would occur.

The depth of the recessed space does not influence the average mass flow rates and average temperatures, for the buoyant flow and the average temperature of air entering all condenser units. In addition, when the depth of the recessed space is changed, the bulk stream remains nearby the condenser units and the corner wall. However, the depth of the recessed space influences flow and temperature distributions inside the upward stream. Because of this, the temperature and mass-flow rates of air in particular condenser units are changed.

The presence of one plate inside the recessed space would cause the overall excess temperature at condenser entrance to fall up to 30%. The presence of two plates would make this figure to be around 40%. When a horizontal plate is provided inside the recessed space at half of its height, performances of WACs would benefit. The presence of the plate would cause the hot air plume to flow out of the recessed space at its half height rather than rising up further. This research has showed that a simple provision of one horizontal plate will decrease an exposure of WACs in the recessed space to higher temperatures by up to 30%. Although the temperature rises for the two topmost levels below the plate could become quite serious, the plate could lead to very significant drop in the temperature rise for many floors above.

References

Anonymous (2000) *Fluent Version 4.23*, Users Manual Fluent Inc., Lebanon, NH, USA.

Bojic, M., Lee, M. and Yik, F. (2001) 'Flow and temperatures outside a high-rise residential building due to heat rejection by its air-conditioners', *Energy and Buildings*, Vol. 33, pp.737–751.

Bojic, M., Lee, M. and Yik, F. (2002) 'Influence of a depth of a recessed space to flow due to air-conditioner heat rejection', *Energy and Buildings*, Vol. 34, pp.33–43.

Bojic, M., Yik, F. and Lee, M. (2003) 'Influence of plates on flow inside a recessed space generated by rejected heat', *Building and Environment*, Vol. 38, pp.593–604.

Chen, Q. and Jiang, Z. (1992) 'Significant questions in predicting room air motion', *ASHRAE Transactions*, Vol. 98, pp.929–939.

Chow, T.T. and Lin, Z. (1999) 'Prediction of on-coil temperature of condensers installed at tall building re-entrant', *Applied Thermal Engineering*, Vol. 19, pp.117–132.

Chow, T.T., Lin, Z. and Wang, Q.W. (2000) 'Effect of building re-entrant shape on performance of air cooled condensing units', *Energy and Buildings*, Vol. 32, pp.143–152.

Costa, J.J., Oliveira, L.A. and Blay, D. (1999) 'Test of several versions for the k–ε type turbulence modelling of internal mixed convection flows', *Int. J. Heat and Mass Transfer*, Vol. 42, pp.4391–4409.

Launder, B.E. and Spalding, D.B. (1974) 'The numerical computation of turbulent flows, *Computer Methods in Applied Mechanics and Engineering*, Vol. 3, pp.269–289.

Vandoormaal, J.P. and Raithby, G.D. (1984) 'Enhancements of the simple method for predicting incompressible fluid flows', *Numerical Heat Transfer*, Vol. 7, pp.147–163.

Yik, F. (2000) 'COP of air conditioners as a function of outside and inside temperature', *Topical Report of the Hong Kong Polytechnic University*.